ORIGINAL RESEARCH

Comprehensive Clinical Diagnostic Pipelines Reveal New Variants in Alpha-1 Antitrypsin Deficiency

Stefania Ottaviani[1], Giulia Bartoli[2], Tomás P. Carroll[3], Fabrizio Gangemi[2], Alice M. Balderacchi[1], Valentina Barzon[4], Alessandra Corino[1], Davide Piloni[1], Noel G. McElvaney[3], Angelo G. Corsico[1,4,5], James A. Irving[6], Annamaria Fra[2]*, and Ilaria Ferrarotti[1,4,5]*

[1]Centre for Diagnosis of Inherited Alpha-1 Antitrypsin Deficiency, Unità Operativa Complessa Pneumologia, Fondazione Istituto di Ricovero e Cura a Carattere Scientifico Policlinico San Matteo, Pavia, Italy; [2]Experimental Oncology and Immunology, Department of Molecular and Translational Medicine, University of Brescia, Brescia, Italy; [3]α-1 Foundation Ireland, Irish Centre for Genetic Lung Disease, Royal College of Surgeons in Ireland Education and Research Centre, Beaumont Hospital, Dublin, Ireland; [4]Department of Internal Medicine and Therapeutics, Pulmonology Unit, University of Pavia, Pavia, Italy; [5]European Reference Network on Rare Respiratory Diseases (ERN-LUNG); and [6]University College London Respiratory, Rayne Institute and the Institute of Structural and Molecular Biology, University College London, London, United Kingdom

ORCID IDs: 0000-0002-2039-230X (S.O.); 0000-0001-8772-1852 (G.B.); 0000-0002-0418-1641 (T.P.C.); 0000-0001-9389-651X (F.G.); 0000-0003-0714-1087 (A.M.B.); 0000-0003-1582-6887 (V.B.); 0000-0002-7275-4229 (D.P.); 0000-0002-0152-4370 (N.G.M.); 0000-0002-8716-4694 (A.G.C.); 0000-0003-3204-6356 (J.A.I.); 0000-0002-4327-3004 (A.F.); 0000-0003-4892-4192 (I.F.).

Abstract

Alpha-1 antitrypsin deficiency (AATD) is an underdiagnosed disorder associated with mutations in the *SERPINA1* gene encoding alpha-1 antitrypsin (AAT). Severe AATD can manifest as pulmonary emphysema and progressive liver disease. Besides the most common pathogenic variants S (E264V) and Z (E342K), many rarer genetic variants of AAT have been found in patients and in the general population. Here we report a panel of new *SERPINA1* variants, including 4 null and 16 missense alleles, identified among a cohort of individuals with suspected AATD whose phenotypic follow-up showed inconclusive or atypical results. Because the pathogenic significance of the missense variants was unclear purely on the basis of clinical data, the integration of computational, biochemical, and cellular studies was used to define the associated risk of disease. Established pathogenicity predictors and structural analysis identified a panel of candidate damaging mutations that were characterized by expression in mammalian cell models. Polymer formation, intracellular accumulation, and secretory efficiency were evaluated experimentally. Our results identified two AAT mutants with a Z-like polymerogenic severe deficiency profile (S_{milano} and $M_{campolongo}$) and three milder variants ($X_{sarezzo}$, P_{dublin}, and $C_{tiberias}$). Overall, the experimentally determined behavior of the variants was in agreement with the pathogenicity scores of the REVEL (an ensemble method for predicting the pathogenicity of rare missense variants) predictor, supporting the utility of this bioinformatic tool in the initial assessment of newly identified amino acid substitutions of AAT. Our study, in addition to describing 20 new *SERPINA1* variants, provides a model for a multidisciplinary approach to classification of rare AAT variants and their clinical impact on individuals with rare AATD genotypes.

Keywords: serpins; serpinopathies; alpha-1 antitrypsin polymers; *SERPINA1* rare variants; pathogenicity predictions

(Received in original form December 13, 2022; accepted in final form April 18, 2023)

*Co–senior authors.

Supported in part by a grant from the Alpha-1 Foundation (to A.F.; ID: 829920), by the Italian Association Alfa1-AT (to A.F.), by Fondazione Cariplo (2013-0967 to A.F. and I.F.), and by the crowdfunding campaign We Breathe Life 2.0 (https://universitiamo.eu/campaigns/respiriamo-la-vita-2-0/; to S.O., A.G.C., and I.F.).

Author Contributions: I.F., A.F., and S.O. designed the research project. T.P.C., I.F., and D.P. collected clinical data. S.O., G.B., F.G., A.M.B., V.B., A.C., and A.F. performed experiments. F.G., J.A.I., and A.F. performed structural analysis. S.O., F.G., J.A.I., and I.F. analyzed data. T.P.C., A.M.B., V.B., A.C., D.P., J.A.I., N.G.M., and A.G.C. critically reviewed the manuscript. S.O., J.A.I., A.F., and I.F. wrote the paper. All authors read and approved the manuscript.

Correspondence and requests for reprints should be addressed to Ilaria Ferrarotti, Ph.D., Centre for Diagnosis of Inherited Alpha-1 Antitrypsin Deficiency, Unità Operativa Complessa Pneumologia, Fondazione Istituto di Ricovero e Cura a Carattere Scientifico Policlinico San Matteo, V.le Taramelli 19, 27100, Pavia, Italy. E-mail: i.ferrarotti@smatteo.pv.it.

This article has a data supplement, which is accessible from this issue's table of contents at www.atsjournals.org.

Am J Respir Cell Mol Biol Vol 69, Iss 3, pp 355–366, September 2023

Originally Published in Press as DOI: 10.1165/rcmb.2022-0470OC on April 18, 2023
Internet address: www.atsjournals.org

Clinical Relevance

We show the benefits of enhancement to a routine diagnostic pipeline with genotyping against an extended panel of disease-associated variants, selective gene sequencing, in silico pathogenicity prediction and selective cellular assays. We report 20 novel variants of the *SERPINA1* gene discovered through the Italian and Irish targeted detection programs for alpha-1 antitrypsin deficiency. We applied established algorithms to predict those mutations most likely to affect the integrity of the alpha-1 antitrypsin protein and evaluated these variants in a mammalian cellular expression system.

Alpha-1 antitrypsin (AAT) is a circulating serpin (serine protease inhibitor) mainly synthesized and secreted by hepatocytes. The AAT protein is encoded by the *SERPINA1* gene within the protease inhibitor locus (14q31-32.3), which spans 12.2 kb and contains five exons and four introns (1). Pathogenic mutations in this gene cause the monogenic disorder alpha-1 antitrypsin deficiency (AATD) (OMIM 613490). People with AATD exhibit insufficient AAT activity in the plasma due to reduced circulating concentrations and/or reduced functional activity. The main role of AAT is inhibition of human neutrophil elastase, and its deficiency leads to a substantially increased risk of lung diseases, including emphysema, chronic obstructive pulmonary disease, and bronchiectasis, primarily because of the uncontrolled proteolytic activity of human neutrophil elastase on the lung parenchyma (2, 3). In addition, some AAT variants are present in the lung as inactive polymeric chains that either derive from circulating polymers secreted into the bloodstream by hepatocytes (4, 5) or may form locally within the lungs as a result of local inflammation and exposure to cigarette smoke (6). AATD may also manifest with liver disease, such as neonatal hepatitis, cirrhosis, and an increased risk of hepatocellular carcinoma. Liver damage is mediated by conformational defects of the AAT mutants leading to formation of polymer chains (7) in the endoplasmic reticulum (ER) of hepatocytes and concomitant accumulation as inclusion bodies (8). Extrapulmonary manifestations of AATD include panniculitis and vasculitis, the underlying pathogenesis of which remains poorly understood (9, 10).

An ever-increasing spectrum of mutations have been identified in the *SERPINA1* gene that yield AAT variants associated with deficiency and that exhibit dysfunctional behavior. The canonical naming of AAT variants reflects their separation by isoelectric focusing (IEF), in which the first letters of the alphabet are used for anodal migration and the last letters denote cathodal migration, occasionally appended by the birthplace of the index case (11, 12). Although convenient for phenotyping, the isoelectric point is not intrinsically reflective of pathogenicity. By convention, amino acid mutations are designated by the residue number in the mature secreted protein, lacking the 24 N-terminal residues of the signal peptide. This system, however, differs from that recommended by the Human Genome Variation Society, in which numbering begins at the initiation methionine (13).

SERPINA1 gene variants can be classified according to their plasma level and/or antielastase activity as normal, deficient, null, or dysfunctional (1). A large number of these, including the most common M alleles (M1, M2, M3, M4, M5) and many rare variants, are characterized by AAT plasma levels that fall within general population reference ranges and are not associated with an increased risk of lung or liver disease (14). Null variants, conventionally designated by "Q0," are characterized by an absence of detectable AAT in the plasma by routine laboratory quantification and are associated with an increased risk of developing emphysema. In most cases, these mutations are generated by premature stop codons, splicing site alterations, insertions, or large deletions (15). An emerging class of AAT variants is found at the other extreme, composed of a subset of coding variants whose plasma levels fall within the normal range but exhibit abnormal antiprotease function (16).

Of the pathogenic missense variants associated with AATD, S (E264V) and Z (E342K) are the most common, but there is also a wide spectrum of rare AAT variants that fall into this category (14, 17). These deficiency variants are characterized by reduced AAT plasma levels and intrahepatic accumulation and are phenotypically associated with an increased risk of developing lung and/or liver disease. The pathogenetic mechanisms of intracellular accumulation have been investigated mainly for the Z AAT mutant. A single mutation (E342K) in the breach region of the Z AAT molecule causes it to adopt a misfolded conformation in the ER of hepatocytes, making it a substrate of ER-associated degradation (18). A significant proportion of the misfolded Z AAT mutant escapes the quality control degradation system and assembles through a domain swap mechanism into long polymeric chains that condense as characteristic periodic acid–Schiff–positive and diastase-resistant inclusion bodies within the ER (8). For the rare variants that have been investigated experimentally, such as M_{malton}, $M_{procida}$, $M_{wurzburg}$, P_{lowell}, I, and $P_{brescia}$, the balance between secretion, degradation, and aggregation determines their pathogenic potential.

Here, we show the benefits of enhancement to a routine diagnostic pipeline with genotyping against an extended panel of disease-associated variants, selective gene sequencing, *in silico* pathogenicity prediction, and selective cellular assays. We report 20 novel variants of the *SERPINA1* gene discovered through the Italian and Irish targeted detection programs for AATD. We applied established algorithms to predict those mutations most likely to affect the integrity of the AAT protein, and we evaluated these variants in a mammalian cellular expression system. The distribution of the missense mutations across the protein highlights the susceptibility of the AAT structure to perturbation. Our study provides insights into the multidisciplinary approach required to achieve a precise diagnosis and classification of newly identified rare variants in AATD.

Methods

Clinical Data

Clinical data, obtained from direct observation of clinical charts and reported here in an anonymized form, are part of the Italian Registry of Alpha-1-antitrypsin Deficiency (RIDA1) (ethical approval 0385 on January 14, 2019, by IRCCS Policlinico S. Matteo of Pavia) or the Irish National AATD Registry (Beaumont Hospital Research Ethics Committee number 05-03).

Table 1. Novel Variants Described in the Present Paper

Variant Name	Nucleotide Change (HGVS)	Amino Acid Change (HGVS)	Amino Acid Change (Conventional)	Base Allele	dbSNP
$Q0_{siracusa}$	c. –5 + 1800_1804delC	—	—	M1(Val)	—
$Q0_{sansiro}$	c.1621_1624delC	p.Pro350Ter	P326Ter	M1(Val)	—
$Q0_{firenze}$	c.1747A>T	p.Lys392Ter	K368Ter	M1(Val)	—
$Q0_{foggia}$	c.1750_1752delC	p.Pro393Pro	P369Pfs*5	S	—
M_{asti}	c.709A>G	p.Thr46Ala	T22A	M2 or M2obernburg	rs1243707738
M_{napoli}	c.774C>G	p.His67Gln	H43Q	M1(Val) or M3	rs140744031
P_{darfo}	c.937G>A	p.Glu122Lys	E98K	M1(Val) or M1(Ala)	—
P_{savona}	c.1042G>A	p.Asp157Asn	D133N	M1(Val)	—
M_{monza}	c.1093A>G	p.Thr174Ala	T150A	M1(Val)	rs1450215301
$X_{sarezzo}$	c.1258G>A	p.Glu229Lys	E205K	M1(Val)	—
F_{milano}	c.1310A>C	p.Lys246Thr	K222T	M1(Val)	rs864622054
P_{dublin}	c.1375T>C	p.Tyr268His	Y244H	M1(Val) or M3	—
M_{andria}	c.1448C>A	p.Thr292Asn	T268N	M1(Val)	—
$L_{bressanone}$	c.1453G>A	p.Asp294Asn	D270N	M1(Val)	rs772436715
M_{ancona}	c.1463C>A	p.Thr297Asn	T273N	M1(Val)	rs752776707
$C_{tiberias}$	c.1513A>C	p.Lys314Gln	K290Q	M1(Val)	—
$V_{verceia}$	c.1548C>G	p.Ser325Arg	S301R	M1(Val)	—
S_{milano}	c.1666G>T	p.Asp365Tyr	D341Y	M3	rs143370956
$M_{campolongo}$	c.1793T>C	p.Leu407Pro	L383P	M1(Ala) or M2	—
$X_{magenta}$	c.1822C>A	p.Gln417Lys	Q393K	M2	—

Definition of abbreviation: HGVS = Human Genome Variation Society.
The reference sequence used for the *SERPINA1* transcript annotation is National Center for Biotechnology Information NM_001127701.1, and the reference sequence for the SERPINA1 protein is UniProt P01009. Variants are sorted by gene location.

Biochemical and Molecular Diagnosis of AATD

Biochemical and genetic tests to diagnose AATD were used in this study with the understanding and written consent of each subject, according to each institution's ethical recommendations. Suspected AATD samples underwent a diagnostic algorithm comprising measurement of serum AAT and C-reactive protein; AAT phenotyping by IEF; genotyping for detection of S, Z, and a panel of 14 rare AAT alleles (19); and, where inconclusive, *SERPINA1* gene sequencing by Sanger or next-generation sequencing methods (1, 20).

Pathogenicity Predictions and Structural Analysis

The pathogenic impact of single amino acid variations resulting from missense SNPs was predicted computationally with PolyPhen-2 (21) and REVEL (14, 22). Possible structural consequences were evaluated with reference to native AAT (a hybrid model of Protein Data Bank 3NE4 and 1HP7).

Sequence Conservation Analysis

AAT orthologs 350–450 residues in length from a BLAST search (23) of the UniProtKB database (e-value, ≤0.1) using entry P01009 were pruned with reference to a ClustalOmega (24) tree, with one complete sequence most similar to the human protein retained for each species. Amino acid conservation at sites of interest within the resulting alignment was determined with the Python implementation of WebLogo (25).

Expression Vectors

Expression vectors based on pcDNA3.1/Zeo(+) and encoding M1V and Z AAT were obtained previously (26). New vectors were obtained from M1V by the QuikChange II site-directed mutagenesis kit. Reagents and primers are listed in Tables E1 and E2 in the data supplement.

Cell Transfection and Lysis

HEK 293T/17 (American Type Culture Collection, CRL-11268) and Hepa 1-6 (American Type Culture Collection, CRL-1830) cell lines were cultured in Dulbecco's modified Eagle medium/10% FBS and transiently transfected by polyethylenimine as described previously (27, 28) and in the data supplement. Transfected cells were incubated for 20 hours in Opti-MEM. Culture media were then collected and centrifuged to remove cell debris, and the cells were lysed in a 1% Nonidet P-40 (NP-40) buffer. NP-40–soluble fractions were separated by centrifugation from the insoluble fractions, which were resuspended in equal volumes of lysis buffer and solubilized by sonication.

SDS-PAGE and Immunoblots

Samples in SDS sample buffer/25 mM DTT were separated by 8% SDS-PAGE and transferred onto low-fluorescence polyvinylidene difluoride membranes, and they were subsequently probed with anti-human AAT polyclonal antibody (Dako) and horseradish peroxidase–conjugated anti-rabbit IgG antibody revealed by ECL Plus.

Quantification of AAT

Total and polymeric AAT was quantified by two sandwich ELISA protocols, as described in the data supplement.

Immunofluorescence and Confocal Microscopy

Hepa 1-6 cells grown on glass coverslips overnight were transfected, fixed with 4% paraformaldehyde after 24 hours, permeabilized (5 min in PBS/0.1% Triton X-100), saturated with PBS/0.1% BSA/0.05% Triton X-100, and immunostained with anti-AAT polymer 2C1 mAb (0.5 μg/ml) (29), followed by rabbit anti-human AAT (Dako) (2 μg/ml), and Alexa Fluor–conjugated secondary antibodies. Nuclei were stained

Table 2. Novel Alpha-1 Antitrypsin Variants and Predicted Impacts

Amino Acid Change (HGVS)	REVEL	PolyPhen-2 Hvar-HDiv	Exposure	Domain	Conservation	Structural Features
Null						
P326Ter	n/a	n/a	—	Δs5A/RCL/1C/4B/5B	—	Likely to form a soluble, nonnative molten globule conformation*
K368Ter	n/a	n/a	—	Δs4B/5B	—	Missing the region exchanged in a C-terminal polymer; feasible a proportion may form heterodimer by accepting C-terminus from a full-length variant
P369Pfs*5	n/a	n/a	—	Δs4B/5B	—	As above
Predicted benign						
T22A	0.221	0/0	E	N-terminus		In a region disordered in most 3D structures; alanine predominant in other species
H43Q	0.264	0.002–0.005	E	hA		Mutation-tolerant site
D133N	0.276	0.004–0.033	E	hE		Conservative change expected to maintain weaker polar contact with K129; change in surface charge
T150A	0.285	0.001–0.005	E	hF		Sidechain does not make important contacts; mutation-tolerant site; alanine tolerated in other species
K222T	0.196	0.001–0.162	E	s3C		Loss of stabilizing salt bridge between strands 3C/4C; site tolerant of polar substitutions in other species
T268N	0.240	0.018–0.216	E	—		Polar substitution at a site that stabilizes helix H by a hydrogen bond; asparagine seen in other species, so conservative change likely maintains contacts
D270N	0.167	0.080–0.083	E	hH		Conservative substitution; sidechain does not make important contacts
T273N	0.085	0.003–0.109	E	hH		Sidechain does not make important contacts

(*Continued*)

Table 2. (*continued*)

Amino Acid Change (HGVS)	REVEL	PolyPhen-2 Hvar-HDiv	Exposure	Domain	Conservation	Structural Features
S301R	0.227	0–0	E	hI		Sidechain not involved in important contacts; change in surface charge
Q393K	0.161	0.004–0.033	E	—		Polar substitution of sidechain that does not make important contacts; change in surface charge
Predicted damaging E98K	0.392	0.004–0.015	E	hD		Breaks intrahelix D salt bridge, minimal effects on stability expected; polar amino acid mutation-tolerant site; change in surface charge
E205K	0.217	0.219–0.169	E	s4C		Sidechain does not make important contacts; change in surface charge
Y244H	0.798	1–1	B	s2B		Packs against conserved positions 190 and 194; charged polar replacement expected to destabilize the functionally important breach region: tendency toward polymerization and some effects on inhibitory activity might be expected; highly conserved site
K290Q	0.569	0.326–0.948	E	—		Highly conserved site; loss of salt bridge to conserved position 342; K290E mutation at this site did reduce secretion* with effect on polymerization unknown
D341Y	0.648	0.002–0.005	E	s5A		Located immediately C-terminal to strand 5A in a region sensitive to destabilization, associated with polymer formation*; loss of highly conserved residue
L383P	0.819	0.004–0.015	B	s5B		Proline forms β-bulge in strand 5B, destabilization of which may promote C-terminal polymerization

Definition of abbreviations: 3D = three-dimensional; n/a = not applicable.
*See References 30, 33, and 34.

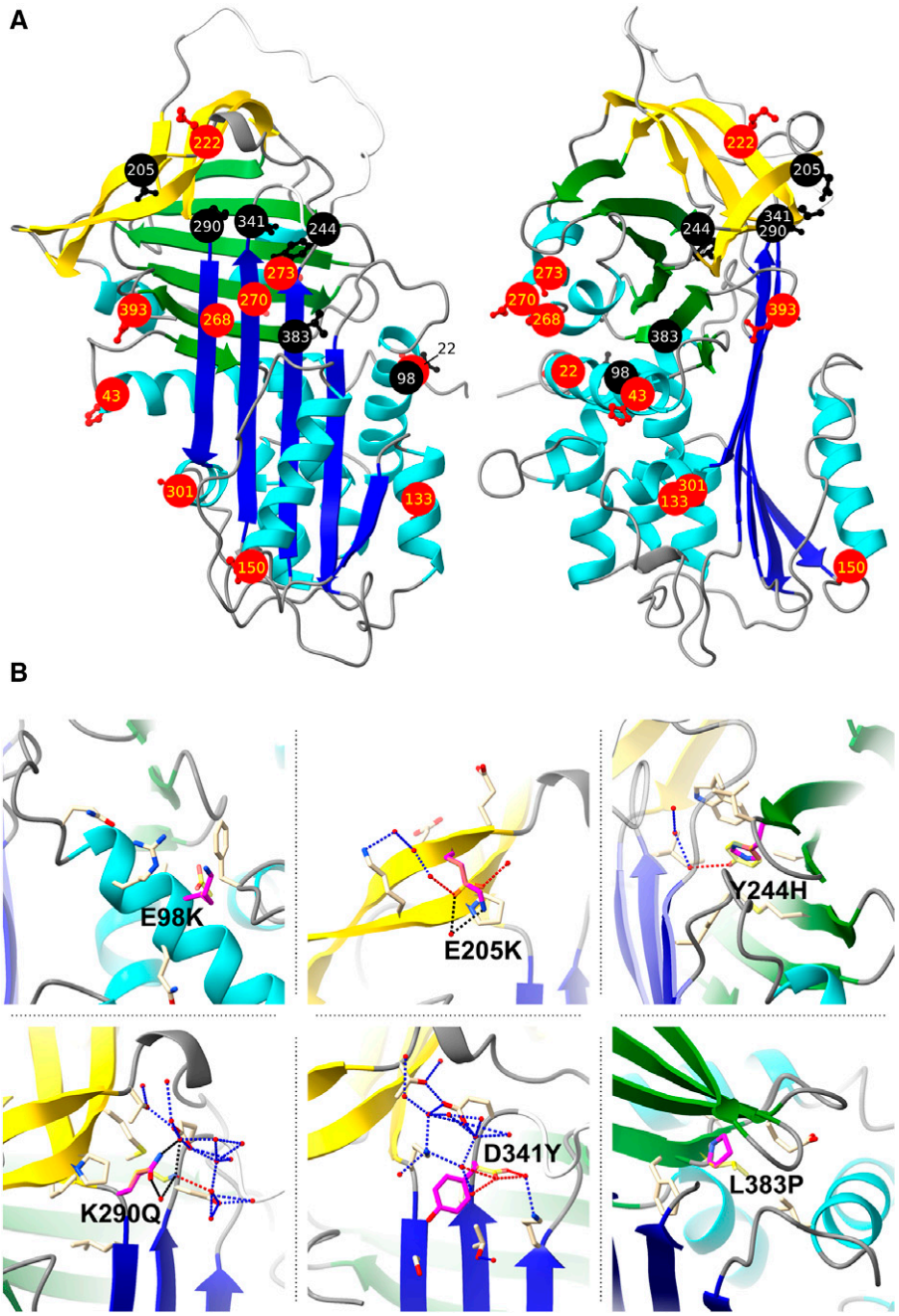

Figure 1. Location of variants identified in this study with reference to native alpha-1 antitrypsin (AAT). (*A*) Predicted minimally perturbing (red) and perturbing (black) variants, mapped onto the structure of AAT reconstructed from Protein Data Bank entries 1HP7 and 3NE4. (*B*) Detailed views of residues predicted to be perturbing are also shown, in which the wild-type residue is shown in dark yellow stick, the mutation in magenta stick, nearby residues are pale yellow, and water molecules are red spheres. Polar interactions present in both the wild-type and mutant are shown as dashed blue lines, those present only in the wild type are red, and those only in the mutant are yellow; black dashes indicate an altered but preserved bond. Secondary structure elements are β-sheets A (blue), B (green), and C (yellow), with helices in cyan and loop regions gray.

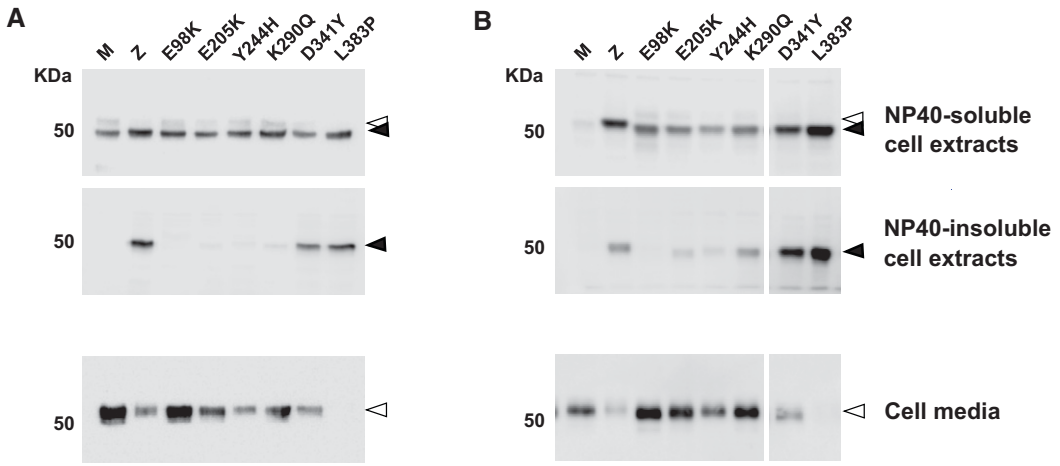

Figure 2. Characterization of AAT variants in cell models. HEK293T (*A*) and Hepa 1-6 (*B*) cells were transfected to express the indicated AAT variants and incubated for 24 hours in serum-free Opti-MEM. The cell culture media were collected, and the cells were lysed in 1% vol/vol Nonidet (NP)-40 buffer. NP-40–soluble material was separated by centrifugation from insoluble material containing nuclei and AAT polymer aggregates. The latter was resuspended and sonicated, and both cellular fractions were separated in 8% SDS-PAGE and detected by immunoblot with an anti-AAT polyclonal antibody (Dako). Black and white arrowheads indicate high mannose and complex N-glycosylated forms of AAT, respectively.

with DAPI. Coverslips were mounted with ProLong mountant and analyzed on a Zeiss LSM510 confocal microscope.

Results

Novel SERPINA1 Allelic Variants

During the diagnosis of individuals referred to the Centre for Diagnosis of Inherited Alpha-1-Antitrypsin Deficiency (Pavia, Italy) or the Alpha-1 Foundation Ireland, Beaumont Hospital (Dublin, Ireland) for suspected AATD, we identified 20 novel allelic variations in the *SERPINA1* gene, comprising 4 null mutations and 16 missense SNPs (Table 1). None had been described previously. Genetic, biochemical, and clinical data on the probands are reported in the data supplement and Table E3 for each variant and are summarized in Table 1.

Pathogenicity Predictions and Structural Analysis

The occurrence of newly identified AAT variants in simple or compound heterozygosity and their variable presentation substantially limits the interpretation of their phenotypic impact on the carriers. Several bioinformatic tools have been developed to help predict the functional effects of coding variations, based on analysis of conservation in multiple sequence alignments, the biochemical properties of amino acid substitutions, and the impact on three-dimensional structures of the affected protein.

We subjected the 16 newly identified AAT missense variations to two pathogenicity prediction algorithms, Polyphen-2 (21) and REVEL (22), to predict their pathogenic significance and to prioritize them for characterization in cellular models (Table 2). Although Polyphen-2 is widely used, the REVEL algorithm emerged as the best-performing predictor of pathogenicity for *SERPINA1* nonsynonymous polymorphisms (14); in that work, Giacopuzzi and colleagues defined three groups that optimize classification on the basis of cluster analysis of REVEL scores: cluster 1 identifies the likely benign AAT variants (0–0.354) and cluster 3 the probably pathogenic ones (0.618–1), whereas cluster 2 (0.355–0.618) includes variants with milder or uncertain significance.

Applying these cutoff values, the majority of the new variants were predicted as neutral (score, <0.355), two variants (E98K and K290Q) produced intermediate scores (0.355–0.618), and three AAT variants (Y244H, D341Y, and L383P) were classified as deleterious (score, >0.618). Polyphen-2, which classifies as benign the substitutions with a score below 0.15, provided similar results but also predicted the E205K variant as possibly damaging.

To extend our analysis, the localization and intramolecular interactions of the mutated residues were evaluated using the native AAT structure (Figure 1A) with additional reference to patterns of conservation among putative AAT orthologs across 82 species (Table 2).

Truncation variants Three out of four identified null variants are the result of mutations that cause a loss of key C-terminal structural elements. P326Ter ($Q0_{sansiro}$) lacks strands 5A, 1C, 4B, and 5B and the reactive center loop. In a study of the folding properties of AAT fragments, one that incorporated a near-identical residue range (1–323) was found to be soluble and behave as a molten globule folding intermediate (30), and therefore, in a cellular context, it may elicit the unfolded protein response and would certainly contribute to the degradative burden. Both K368Ter ($Q0_{firenze}$) and P369Pfs*5 ($Q0_{foggia}$) lack strands 4B and 5B that are required for positioning of the reactive center loop and strand 1C in the native state. There is evidence that an AAT molecule lacking an incorporated C-terminus is unable to undergo the self-insertion process (30) that is believed to be central to the polymerization mechanism (8). By analogy to the heteropolymerization of Z with M and S variants, it is conceivable that a proportion of these molecules may capture coexpressed variants as heterodimers (31, 32).

Because of the intronic localization of the $Q0_{siracusa}$ (c.-5 + 1800_1804 delC), we cannot provide a similar analysis. Because this nevertheless results in an absence of

AAT, we conclude that the deletion may directly affect a splicing site.

Likely benign variants. The variants predicted to be benign are largely surface exposed, mediating either no or minimal observed interactions with other structural elements, and in sites generally found to be polymorphic in orthologs across species (Figure E1). *Q393K* ($X_{magenta}$) and T22A (M_{asti}) are located in regions of the AAT structure that are disordered in at least some crystal structures and are at sites tolerant of substitutions in orthologs (Table 2). Similarly, H43Q (M_{napoli}), T150A (M_{monza}), D270N ($L_{bressanone}$), T273N (M_{ancona}), and S301R ($V_{verceia}$) are at positions that do not make important contacts with other residues. Others show conservative polar substitutions that are expected to retain similar interactions. Position 133, sited within helix E, forms a polar contact with K129, which would be expected to be maintained in the D133N (P_{savona}) variant; T268N (M_{andria}) is similarly predicted to maintain a network of polar interactions at the N-terminal end of helix H. The substitution in this category most likely to have a structural impact, K222T (F_{milano}), results in a loss of a salt bridge that contributes to the interface between 3C and 4C, but the site is generally tolerant of polar substitutions among orthologs and is thus unlikely to significantly perturb AAT structure.

Potentially damaging variants. Four of the six variants with high REVEL/Polyphen scores all arise in the vicinity of the AAT "breach" region (Figure 1B). K290Q ($C_{tiberias}$) is proximate to the location of the Z mutation, E342; although it had been hypothesized in early studies that loss of a 290–342 salt bridge would contribute to the polymerogenic behavior of Z, the partial tolerance of this site to mutagenesis is demonstrated by a K290E mutation that reduced secretion in a cell model by only approximately one-third (33). This modest effect is consistent with its intermediate REVEL score.

The strictly conserved Y244 side chain is integral to the "breach" region at the top of β-sheet A that is the site of incorporation of the reactive center loop during the inhibition of a target protease. Destabilization of this region in the presence of the pathogenic Z mutation causes AAT to adopt the M* intermediate with solvation of a cryptic pocket (34). In the Y244H (P_{dublin}) variant, the histidine side chain would maintain a polar character but perturb the water-bonding network of the breach (Figure 1B). A molecular dynamics simulation, performed to investigate the possible consequences in more detail, suggests that changes to the local interaction network, including new interactions that are established between the NH group on the ring of H244 and the backbone atoms of G192 and K193, likely are the cause of a structural alteration of a strand of β-sheet A (Figures E2 and E3).

D341Y (S_{milano}) also represents the substitution of a strictly conserved residue. Loss of this residue disrupts a network of water-mediated interactions at a site directly preceding position 342 of the Z mutation (Figure 1B). This might be expected to partially destabilize the top of strand 5A, a factor that is known to result in polymerization (34). Indeed, in molecular dynamics simulations, analysis of the network of local interactions of the wild-type protein shows that D341, as well as E342, because of its negatively charged side chain, has a crucial role in the stability of the upper end of strands s5A and s6A in β-sheet A as well as the hinge region between residues 340 and 344 (Figure E4).

L383P ($M_{campolongo}$), situated in β-strand 5B, is buried adjacent to the "breach" region and the cryptic pocket that is revealed in the M* intermediate (35, 36). The replacement of leucine by proline would alter the hydrophobic packing of this region, and the stereochemical constraints imposed on the backbone by the proline residue would additionally be expected to partially destabilize the local β-strand conformation. Because this element is involved in an intermolecular domain swap during C-terminus–mediated polymerization (7), a destabilized C-terminus could result in displacement of this region and therefore polymer formation.

Inspection of the E98K (P_{darfo}) and E205K ($X_{sarezzo}$) variants makes their relatively high scores somewhat surprising because, in the native structure, they are surface exposed and lack a clear interaction with other residues, although they would alter the local surface charge.

These observations collectively suggest that the mutations most likely to result in pathogenic outcomes are situated in the vicinity of the breach region. We chose these four residues, as well as the two others with intermediate pathogenicity scores, for further experimental characterization.

Characterization of the AAT Variants Expressed in Cellular Models

Intracellular polymerization. The variants selected by our preliminary bioinformatic and structural evaluation were expressed and characterized in both the HEK293T and the Hepa 1-6 cell lines, with wild-type M and the polymerogenic Z AAT mutants used for reference. Polymer formation was first assessed by the tendency of the proteins to accumulate as intracellular aggregates resistant to NP-40 treatment (37).

Cells were transiently transfected and cell media and extracts that were soluble or insoluble by 1% vol/vol NP-40 treatment, were evaluated by SDS-PAGE and immunoblot (Figure 2). As expected for a readily secreted protein, M AAT was exclusively present in the detergent-soluble fraction, and a similar profile was observed for the E98K AAT variant in both cell lines. Polymerogenic Z AAT was distributed approximately equally between the NP-40–soluble and NP-40–insoluble fractions, and a similar profile was observed for the D341Y and L383P variants. Traces of NP40-insoluble polymers were detected in the E205K, Y244H, and K290Q variants. Analysis of the AAT variants in the cell media showed a marked deficiency of Z as well as of the polymerogenic D341Y and L383P.

Secretion profile. The impact of the mutations on secretion efficiency was evaluated by quantifying AAT in the culture media of both HEK293T and Hepa 1-6 transfected cells by sandwich ELISA (Figure 3). Consistent with previous studies (26, 31, 38), the Z variant was secreted significantly less than wild-type M AAT. In comparison, E98K was secreted at nearly normal levels, L383P showed the most severe reduction, a moderate reduction was observed for D341Y, and a milder but significant deficiency was observed for the other variants. Strikingly, when the secretion levels of the AAT variants were plotted against their REVEL scores (Figure 3, right panels), a common trend was observed, supporting the potential of this algorithm to prospectively predict deficiency and associated disease risk.

Accumulation of Polymerogenic Mutants within Inclusion Bodies

A fraction of polymerogenic variants can be secreted as polymers (5). To determine whether there was any direct evidence of polymer formation by the novel variants, we

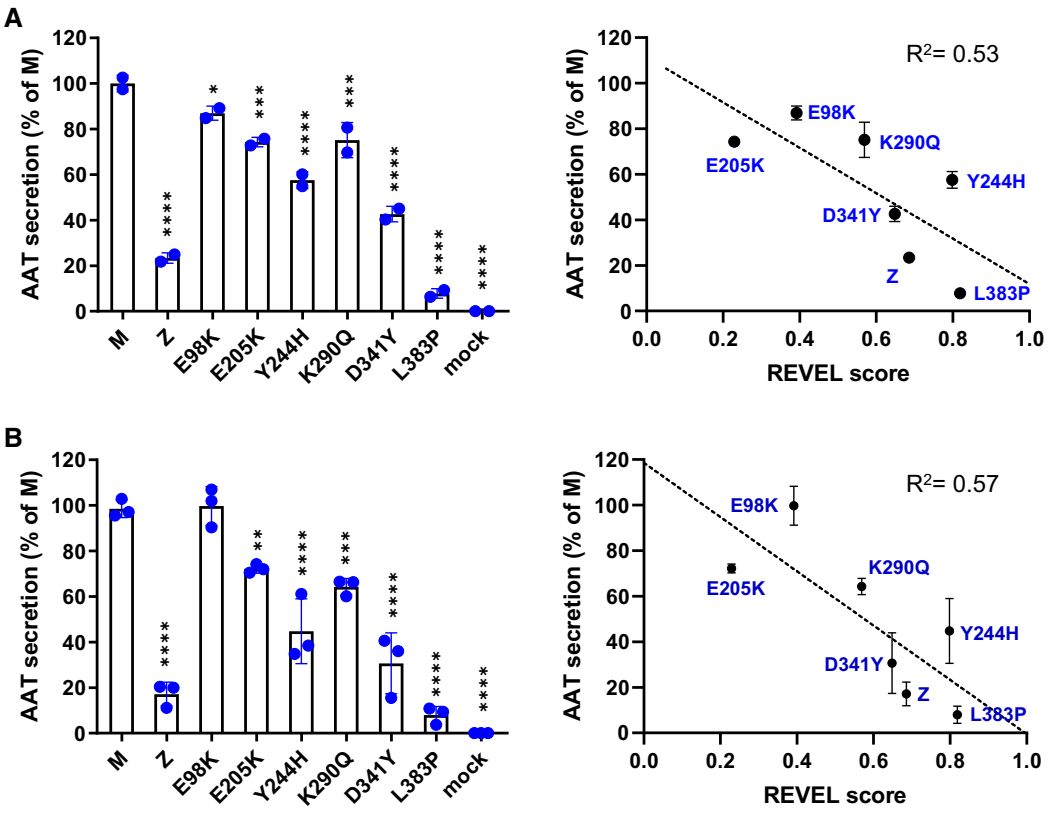

Figure 3. Secretion efficiency of the novel AAT variants. Total AAT levels in the cell media of HEK293T (*A*) or Hepa 1-6 (*B*) transfected cells were measured by ELISA and represented as the percentage of the wild-type M levels (left) (mean ± SD, with experimental values as blue circles; $n = 2$ and $n = 3$ independent transfection experiments for HEK293T and Hepa 1-6, respectively) (one-way ANOVA, $P < 0.0001$; Dunnett's multiple comparison test between each variant and M AAT, $^{*}P < 0.05$, $^{**}P < 0.01$, $^{***}P < 0.001$, $^{****}P < 0.0001$). Secretion AAT levels for each variant were plotted versus the REVEL (an ensemble method for predicting the pathogenicity of rare missense variants) score assigned to the variant (right), and correlation was determined by linear regression ($R^2 = 0.53$ for HEK293T and $R^2 = 0.57$ for Hepa 1-6).

evaluated their presence in the cell media by a sandwich ELISA based on the monoclonal antibody 2C1. This experiment revealed detectable polymer formation by D341Y and L383P (Figure 4A).

Intracellular accumulation and distribution of these polymerogenic AAT variants were subsequently investigated by immunofluorescence staining and confocal microscopy. Wild-type M, the polymerogenic Z AAT, and D341Y and L383P were transiently expressed in Hepa 1-6 cells, and the cells were fixed and stained with the polymer-specific 2C1 mAb and the anti-total AAT polyclonal antibody (Figure 4B). As expected, wild-type M AAT was only recognized by the nonconformation selective polyclonal antibody, with a reticular staining pattern and a perinuclear localization, consistent with accumulation within the Golgi apparatus. Z AAT resulted in the formation of 2C1-positive punctate structures resembling the inclusion bodies previously reported in cellular models expressing Z AAT (29, 39). Similar patterns were seen for the D341Y and L383P variants, thus confirming their propensity to accumulate Z-like, 2C1-positive polymers within the cell.

Discussion

With developments in clinical pipelines and advances in genomic technologies, an ever-increasing number of rare AAT variants are being identified. Many rare variants are not easily diagnosed with routine laboratory techniques, thus contributing to misclassification and misdiagnosis. For example, phenotyping by IEF usually does not allow the precise identification of M-like AAT variants, such as M_{malton} and $M_{procida}$ (40), because they are easily confused with M (normal) protein. Furthermore, Null (Q0) variants in heterozygosity are invisible to IEF and can be observed only indirectly through their effects on circulating levels. Most rare alleles can be detected only by molecular biology techniques, such as *SERPINA1* gene sequencing (1, 41). Sometimes, depending on the complexity of the case, sequencing of exons might not be sufficiently informative, and more extensive analysis by whole-gene sequencing is required to detect rare exonic deletions, alterations in promoters, or deep intronic regions not covered by standard sequencing (9, 40). It has recently been demonstrated that the choice of diagnostic algorithm can have a significant impact on the accurate diagnosis of AATD, which is essential for appropriate medical care and treatment (42). This is exemplified by the finding of the $Q0_{foggia}$ mutation, described herein, that is *in cis* with an S allele: A simpler diagnostic algorithm that includes

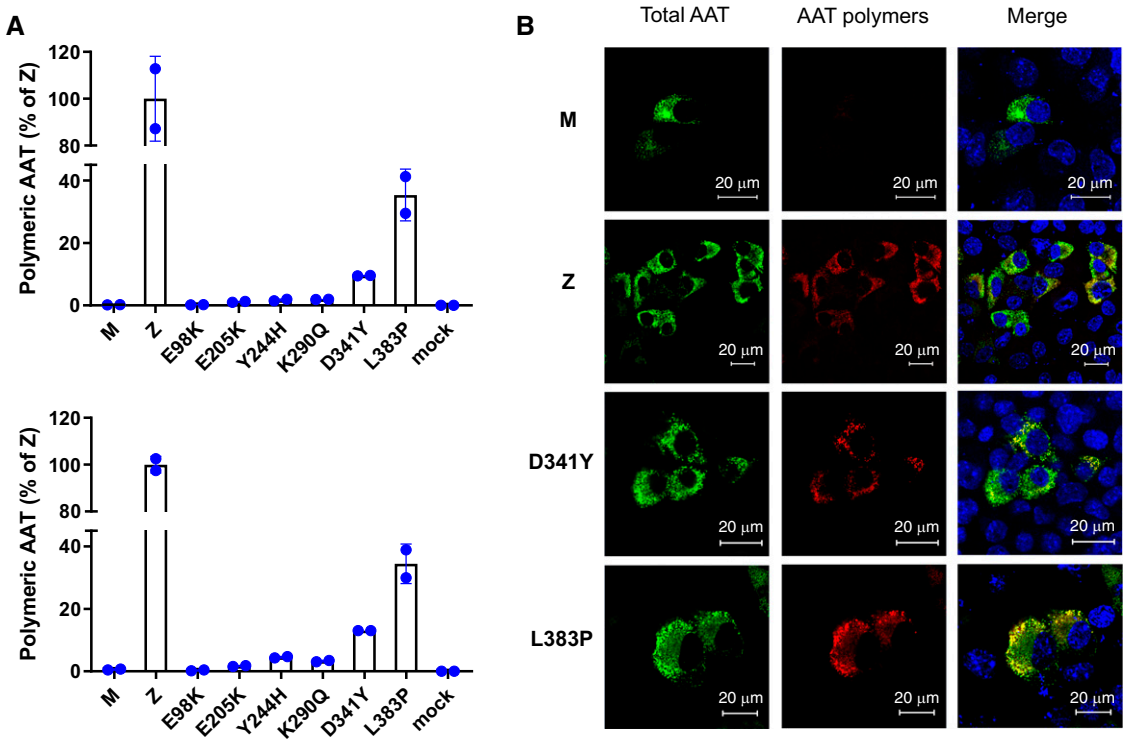

Figure 4. Mutant variants of AAT accumulate 2C1-positive polymers. (*A*) Polymeric AAT in the cell media of transfected HEK293T (top) and Hepa 1-6 (bottom) cells were measured by a sandwich ELISA based on mAb 2C1 capture, normalized to total AAT levels, and represented as the percentage of Z AAT polymer levels (mean ± SD with experimental values as blue circles, $n = 2$ independent transfections for both HEK293T and Hepa 1-6). (*B*) Hepa 1-6 cells seeded on glass coverslips were fixed with 4% paraformaldehyde 24 hours after transfection with the wild-type M AAT, the polymerogenic mutant Z AAT, and D341Y and L383P AAT variants. After permeabilization, cells were stained with the anti-AAT polymer 2C1 mAb (red) and a rabbit anti-human AAT polyclonal antibody (Dako) (green), detected with goat anti-mouse IgG secondary antibody conjugated to Alexa Fluor 594 and goat anti-rabbit antibody conjugated to Alexa Fluor 488, respectively. Images were acquired on a Zeiss LSM510 confocal microscope with a 63× objective (1.4 oil). Scale bars, 20 μm.

only the detection of most common variants would have identified a low-risk S variant rather than a high-risk null allele.

Precise identification of the AAT genotype facilitates the accurate clinical management of a patient, but for variants that are uncharacterized or with conflicting evidence for pathogenicity, this must be interpreted through the lens of molecular pathological mechanisms: Diagnostic procedures should provide this combined information to clinicians. Virtually all *SERPINA1* nonsense mutations will have a deleterious effect due to lack of protein synthesis, severe effects on the folding and stability of the protein, or lack of activity: There is no dispensable C-terminal component to the AAT structure. Therefore, individuals with a novel null variant should always be considered at particularly high risk of emphysema within the spectrum of AATD, with a prognosis similar to that of other previously reported null alleles (15, 43).

Unlike null, the molecular mechanisms of missense variants are more variable, and the pathogenicity of novel missense variants cannot be inferred by clinical data gathered from a single individual (44, 45). The presumption of a "benign" or "pathogenic" mutation without robust supporting evidence risks inappropriate management of AATD. Misinterpretation of novel variant(s) can lead to inappropriate diagnostic calls and clinical care.

Several bioinformatic tools have been developed to streamline the functional assessment of newly identified protein coding variants, based on multiple features such as amino acid or nucleotide conservation, the biochemical properties of amino acid substitutions, and structural data. REVEL is an ensemble predictive method that performed best in discriminating known pathogenic AAT variants from those classified as benign (14). In the present study, we found that REVEL showed a good correlation with the level of secretion exhibited by variants in the two mammalian expression systems used.

Cellular models of disease have proved to be good correlates with clinical manifestations of deficiency alleles by recapitulating the consequences of misfolding, degradation, and aggregation in a native-like environment. This is generally accomplished by transient transfection in hepatoma cells or in nonhepatic cell lines achieving higher expression levels, such as HEK293T or COS-7 cells (27, 28, 36, 46). Here, we used both Hepa 1-6 and HEK293T cell lines, which revealed similar behavior for each of the variants evaluated: Y244H (P_{dublin}), D341Y (S_{milano}), and L383P ($M_{campolongo}$) showed moderate to severe secretion deficiency, with the latter two also exhibiting marked accumulation of intracellular NP-40–insoluble polymers and 2C1-positive inclusions by confocal microscopy. A milder deficiency was observed for E205K ($X_{sarezzo}$) and K290Q ($C_{tiberias}$). Our results suggest that individuals

with D341Y and L383P variants in heterozygosity with other deficiency variants may have an associated risk of developing both lung and liver dysfunction. The detailed characterization presented here further extends the number of naturally occurring rare mutations in AAT with pathogenic potential that have been identified.

Naturally arising serpin variants have played a key role in the elucidation of mechanisms underlying molecular dysfunction, including polymerization (47). Of the newly described AAT variants, those that are not expected to exhibit a pathogenic phenotype are, for the most part, surface exposed, polar, not involved in interactions with other structural elements, and at sites that are relatively polymorphic among orthologs in other species. Our structural analyses reveal that, collectively, the variants occupy a diversity of positions throughout the molecule; it is therefore striking that those we show to be the most deleterious all occur in proximity to the "breach." This region of the molecule is destabilized in the Z variant (7) and overlies the C-terminal strands s4B and s5B that are displaced to form intermolecular interactions during polymer formation in the liver (8). In addition, the breach is the point of insertion of the reactive center loop during inhibition of a target protease, and, by analogy with the Z variant, these mutations may also result in a reduction of protease inhibitory efficiency.

The results presented here show that routine incorporation of genetic analysis within an AATD diagnostic pipeline can provide important clinical insight that would otherwise escape detection. In the event of an uncharacterized variant being identified, these data further support the usefulness, in the absence of other experimental information, of pathogenicity predictors in establishing the likelihood of a deleterious effect on the protein. This can be augmented by a consideration of the structural context in relation to deficiency "hot spots" in the vicinity of the breach and shutter domains. Ultimately, where possible, the gold standard approach in a research setting remains the evaluation of the variant in a cellular context.

Other members of the serpin superfamily are associated with conformational diseases, called "serpinopathies," associated with misfolding and ordered aggregation, causing conditions ranging from dementia to thrombosis. Our results indicate that pathogenicity predictors are compatible with the idiosyncrasies of the serpin fold, and, accordingly, our approach combining an *in silico* triage with subsequent evaluation of cellular accumulation and export has the potential to benefit diseases arising from molecular defects in related proteins. In a wider context, this paper provides evidence of the usefulness of integration of cellular models, prediction analysis, and clinical data to guide the care of patients with genetic diseases caused by uncharacterized rare mutations. ■

Author disclosures are available with the text of this article at www.atsjournals.org.

Acknowledgment: The authors thank Chiara Masserini for technical assistance and Mattia Laffranchi and Andrea Denardo for discussions. The authors also acknowledge Dr. Christine Seebacherand and Dr. Davide Spadaro for providing clinical data of cases A3 and O1 (Table E3).

References

1. Ferrarotti I, Ottaviani S. Laboratory diagnosis. In: Strnad P, Brantly ML, Bals R, editors. α1-Antitrypsin deficiency (ERS monograph). Sheffield: European Respiratory Society; 2019. pp. 39–51.
2. Greene CM, Marciniak SJ, Teckman J, Ferrarotti I, Brantly ML, Lomas DA, *et al.* α1-Antitrypsin deficiency. *Nat Rev Dis Primers* 2016;2:16051.
3. Strnad P, McElvaney NG, Lomas DA. Alpha$_1$-antitrypsin deficiency. *N Engl J Med* 2020;382:1443–1455.
4. Tan L, Dickens JA, Demeo DL, Miranda E, Perez J, Rashid ST, *et al.* Circulating polymers in α1-antitrypsin deficiency. *Eur Respir J* 2014;43: 1501–1504.
5. Fra A, Cosmi F, Ordoñez A, Berardelli R, Perez J, Guadagno NA, *et al.* Polymers of Z α1-antitrypsin are secreted in cell models of disease. *Eur Respir J* 2016;47:1005–1009.
6. Alam S, Li Z, Janciauskiene S, Mahadeva R. Oxidation of Z α1-antitrypsin by cigarette smoke induces polymerization: a novel mechanism of early-onset emphysema. *Am J Respir Cell Mol Biol* 2011;45:261–269.
7. Yamasaki M, Sendall TJ, Pearce MC, Whisstock JC, Huntington JA. Molecular basis of α1-antitrypsin deficiency revealed by the structure of a domain-swapped trimer. *EMBO Rep.* 2011;12:1011–1017.
8. Faull SV, Elliston ELK, Gooptu B, Jagger AM, Aldobiyan I, Redzej A, *et al.* The structural basis for Z α_1-antitrypsin polymerization in the liver. *Sci Adv* 2020;6:eabc1370.
9. Franciosi AN, Ralph J, O'Farrell NJ, Buckley C, Gulmann C, O'Kane M, *et al.* Alpha-1 antitrypsin deficiency-associated panniculitis. *J Am Acad Dermatol* 2022;87:825–832.
10. Lyons PA, Rayner TF, Trivedi S, Holle JU, Watts RA, Jayne DR, *et al.* Genetically distinct subsets within ANCA-associated vasculitis. *N Engl J Med* 2012;367:214–223.
11. Fagerhol MK, Laurell CB. The Pi system-inherited variants of serum alpha 1-antitrypsin. *Prog Med Genet* 1970;7:96–111.
12. Cox DW, Johnson AM, Fagerhol MK. Report of nomenclature meeting for alpha 1-antitrypsin, INSERM, Rouen/Bois-Guillaume-1978. *Hum Genet* 1980;53:429–433.
13. Richards S, Aziz N, Bale S, Bick D, Das S, Gastier-Foster J, *et al.*; ACMG Laboratory Quality Assurance Committee. Standards and guidelines for the interpretation of sequence variants: a joint consensus recommendation of the American College of Medical Genetics and Genomics and the Association for Molecular Pathology. *Genet Med* 2015;17:405–424.
14. Giacopuzzi E, Laffranchi M, Berardelli R, Ravasio V, Ferrarotti I, Gooptu B, *et al.* Real-world clinical applicability of pathogenicity predictors assessed on SERPINA1 mutations in alpha-1-antitrypsin deficiency. *Hum Mutat* 2018;39:1203–1213.
15. Ferrarotti I, Carroll TP, Ottaviani S, Fra AM, O'Brien G, Molloy K, *et al.* Identification and characterisation of eight novel SERPINA1 null mutations. *Orphanet J Rare Dis* 2014;9:172.
16. Laffranchi M, Elliston ELK, Gangemi F, Berardelli R, Lomas DA, Irving JA, *et al.* Characterisation of a type II functionally-deficient variant of alpha-1-antitrypsin discovered in the general population. *PLoS One* 2019;14: e0206955.
17. Seixas S, Marques PI. Known mutations at the cause of alpha-1 antitrypsin deficiency an updated overview of *SERPINA1* variation spectrum. *Appl Clin Genet* 2021;14:173–194.
18. Patel D, Teckman JH. Alpha-1-antitrypsin deficiency liver disease. *Clin Liver Dis* 2018;22:643–655.
19. Ottaviani S, Barzon V, Buxens A, Gorrini M, Larruskain A, El Hamss R, *et al.* Molecular diagnosis of alpha1-antitrypsin deficiency: a new method based on Luminex technology. *J Clin Lab Anal* 2020;34: e23279.
20. Franciosi AN, Carroll TP, McElvaney NG. Pitfalls and caveats in α1-antitrypsin deficiency testing: a guide for clinicians. *Lancet Respir Med* 2019;7:1059–1067.
21. Adzhubei IA, Schmidt S, Peshkin L, Ramensky VE, Gerasimova A, Bork P, *et al.* A method and server for predicting damaging missense mutations. *Nat Methods* 2010;7:248–249.
22. Ioannidis NM, Rothstein JH, Pejaver V, Middha S, McDonnell SK, Baheti S, *et al.* REVEL: an ensemble method for predicting the pathogenicity of rare missense variants. *Am J Hum Genet* 2016;99:877–885.

23. Altschul SF, Madden TL, Schäffer AA, Zhang J, Zhang Z, Miller W, *et al.* Gapped BLAST and PSI-BLAST: a new generation of protein database search programs. *Nucleic Acids Res* 1997;25:3389–3402.
24. Sievers F, Higgins DG. Clustal omega. *Curr Protoc Bioinformatics* 2014; 48:3.13.1–3.13.16.
25. Crooks GE, Hon G, Chandonia JM, Brenner SE. WebLogo: a sequence logo generator. *Genome Res* 2004;14:1188–1190.
26. Medicina D, Montani N, Fra AM, Tiberio L, Corda L, Miranda E, *et al.* Molecular characterization of the new defective P(brescia) alpha1-antitrypsin allele. *Hum Mutat* 2009;30:E771–E781.
27. Ronzoni R, Berardelli R, Medicina D, Sitia R, Gooptu B, Fra AM. Aberrant disulphide bonding contributes to the ER retention of alpha1-antitrypsin deficiency variants. *Hum Mol Genet* 2016;25:642–650.
28. Fra A, D'Acunto E, Laffranchi M, Miranda E. Cellular models for the serpinopathies. *Methods Mol Biol* 2018;1826:109–121.
29. Miranda E, Pérez J, Ekeowa UI, Hadzic N, Kalsheker N, Gooptu B, *et al.* A novel monoclonal antibody to characterize pathogenic polymers in liver disease associated with alpha1-antitrypsin deficiency. *Hepatology* 2010;52:1078–1088.
30. Dolmer K, Gettins PG. How the serpin α1-proteinase inhibitor folds. *J Biol Chem* 2012;287:12425–12432.
31. Laffranchi M, Berardelli R, Ronzoni R, Lomas DA, Fra A. Heteropolymerization of α-1-antitrypsin mutants in cell models mimicking heterozygosity. *Hum Mol Genet* 2018;27:1785–1793.
32. Laffranchi M, Elliston EL, Miranda E, Perez J, Ronzoni R, Jagger AM, *et al.* Intrahepatic heteropolymerization of M and Z alpha-1-antitrypsin. *JCI Insight* 2020;5:e135459.
33. Sifers RN, Finegold MJ, Woo SL. Alpha-1-antitrypsin deficiency: accumulation or degradation of mutant variants within the hepatic endoplasmic reticulum. *Am J Respir Cell Mol Biol* 1989; 1:341–345.
34. Huang X, Zheng Y, Zhang F, Wei Z, Wang Y, Carrell RW, *et al.* Molecular mechanism of Z α1-antitrypsin deficiency. *J Biol Chem* 2016; 291:15674–15686.
35. Jagger AM, Waudby CA, Irving JA, Christodoulou J, Lomas DA. High-resolution ex vivo NMR spectroscopy of human Z α_1-antitrypsin. *Nat Commun* 2020;11:6371.
36. Lomas DA, Irving JA, Arico-Muendel C, Belyanskaya S, Brewster A, Brown M, *et al.* Development of a small molecule that corrects misfolding and increases secretion of Z α_1-antitrypsin. *EMBO Mol Med* 2021;13:e13167.
37. Ronzoni R, Heyer-Chauhan N, Fra A, Pearce AC, Rüdiger M, Miranda E, *et al.* The molecular species responsible for α_1-antitrypsin deficiency are suppressed by a small molecule chaperone. *FEBS J* 2021;288: 2222–2237.
38. Ronzoni R, Ferrarotti I, D'Acunto E, Balderacchi AM, Ottaviani S, Lomas DA, *et al.* The importance of N186 in the alpha-1-antitrypsin shutter region is revealed by the novel Bologna deficiency variant. *Int J Mol Sci* 2021;22:5668.
39. Chambers JE, Zubkov N, Kubánková M, Nixon-Abell J, Mela I, Abreu S, *et al.* Z-α_1-antitrypsin polymers impose molecular filtration in the endoplasmic reticulum after undergoing phase transition to a solid state. *Sci Adv* 2022;8:eabm2094.
40. Barzon V, Ottaviani S, Balderacchi AM, Corino A, Piloni D, Accordino G, *et al.* Improving the laboratory diagnosis of M-like variants related to alpha1-antitrypsin deficiency. *Int J Med Sci* 2022;23:9859.
41. Rizzo JM, Buck MJ. Key principles and clinical applications of "next-generation" DNA sequencing. *Cancer Prev Res (Phila)* 2012;5: 887–900.
42. Balderacchi AM, Barzon V, Ottaviani S, Corino A, Zorzetto M, Wencker M, *et al.* Comparison of different algorithms in laboratory diagnosis of alpha1-antitrypsin deficiency. *Clin Chem Lab Med* 2021; 59:1384–1391.
43. Fregonese L, Stolk J, Frants RR, Veldhuisen B. Alpha-1 antitrypsin Null mutations and severity of emphysema. *Respir Med* 2008;102:876–884.
44. Mosella M, Accardo M, Molino A, Maniscalco M, Zamparelli AS. Description of a new rare alpha-1 antitrypsin mutation in Naples (Italy): PI*M S-Napoli. *Ann Thorac Med* 2018;13:59–61.
45. Carpagnano GE, Santacroce R, Palmiotti GA, Leccese A, Giuffreda E, Margaglione M, *et al.* A new SERPINA-1 missense mutation associated with alpha-1 antitrypsin deficiency and bronchiectasis. *Lung* 2017;195: 679–682.
46. Matamala N, Lara B, Gomez-Mariano G, Martínez S, Retana D, Fernandez T, *et al.* Characterization of novel missense variants of SERPINA1 gene causing alpha-1 antitrypsin deficiency. *Am J Respir Cell Mol Biol* 2018;58:706–716.
47. Stein PE, Carrell RW. What do dysfunctional serpins tell us about molecular mobility and disease? *Nat Struct Biol* 1995;2:96–113.